

# Colloidally Prepared Nanoparticles for the Synthesis of Structurally Well-Defined and Highly Active Heterogeneous Catalysts\*\*

Birte Jürgens, Holger Borchert, Kirsten Ahrenstorf, Patrick Sonström, Angelika Pretorius, Marco Schowalter, Katharina Gries, Volkmar Zielasek, Andreas Rosenauer, Horst Weller, and Marcus Bäumer\*

Colloidally prepared metal nanoparticles are gaining attention for catalytic applications because of the advanced possibilities to tailor particle size and shape, which are often important factors governing activity and selectivity. In the case of bimetallic catalysts, composition is usually difficult to control by traditional techniques, but by colloidal chemistry the relative portions of the metals in the nanoparticles can be exactly predefined. This approach not only offers the advantage of controlling structure and composition but also allows very high particle loadings. Colloidal nanoparticles with well-defined size and shape have a strong tendency to self-organize into well-ordered and close-packed 2D arrangements.<sup>[1,2]</sup> Thus, it can be expected that depositing colloidal nanoparticles on powder supports or on monolithic structures will yield catalysts with high particle loadings, which would be of interest for various applications in heterogeneous catalysis.<sup>[3–5]</sup>

Until now, ligand-capped nanoparticles have been mainly employed as catalysts in colloidal solutions.<sup>[6–8]</sup> In gas-phase heterogeneous catalysis, however, the ligand shell resulting from the synthesis is usually considered to hinder catalytic activity. Therefore, many studies report the removal of the ligand shell, for example, by thermal pretreatment in an inert or reactive atmosphere.<sup>[9–11]</sup> However, high-temperature pretreatment can poison the particles by leaving residues of ligand decomposition,<sup>[12]</sup> or the well-defined structural properties of the colloidally prepared nanoparticles can be lost as a result of sintering effects.<sup>[13]</sup> Recent investigations of CO oxidation by colloidally prepared Pt nanoparticles revealed

catalytic activity in the presence of a partly intact ligand shell.<sup>[14]</sup> A similar result was observed for benzene hydrogenation with only weakly coordinating surfactants on Pt.<sup>[15]</sup> These results suggest that procedures for the complete removal of the ligand shell do not necessarily have to be applied prior to use.

In the present study, we investigated in more detail the possibility to employ colloidally prepared metal nanoparticles for the preparation of heterogeneous catalysts and to use them directly without calcination or reduction treatments. The results prove that well-defined catalysts with exceptional activities can be obtained with this approach but also reveal that the support may have a strong influence on the activity.

High-quality monodisperse colloidal NiPt nanoparticles (molar ratio 1:1) were prepared with oleylamine and oleic acid as organic stabilizers<sup>[16]</sup> and deposited on  $\gamma$ -Al<sub>2</sub>O<sub>3</sub> and MgO powders. CO oxidation was chosen as a test reaction because increased activity and lower onset temperatures for conversion were reported when alloying Pt with Ni and other transition metals.<sup>[18–21]</sup> This effect was ascribed, on the one hand, to lowering of the desorption temperature of CO, which needs to desorb partially so that adjacent free sites for dissociative adsorption of O<sub>2</sub> become available.<sup>[18,19,21]</sup> On the other hand, Ni binds oxygen more strongly than does Pt,<sup>[22]</sup> so that higher surface coverages and thus better availability of oxygen at lower temperatures can be expected.

Figure 1 shows the results of high-resolution TEM characterization before and after catalysis. The images of the pristine particles deposited on magnesia and alumina show that they are highly crystalline and monodisperse with a mean diameter of approximately 4 nm. According to energy-dispersive X-ray (EDX) analysis (not shown), the molar ratio of Pt to Ni is about 1:1.

Both catalysts were studied with respect to CO oxidation in laboratory reactors under continuous-flow conditions. The data in Figure 2 show the development of conversion with the time on stream at 170 °C. Both systems are catalytically active, but distinctly higher conversion rates (ca. 50×) are observed for the magnesia-supported particles. The turnover frequency (TOF) of about 15 s<sup>−1</sup> measured in this case is exceptionally high. Conventionally prepared Pt catalysts exhibit TOF values below 1 s<sup>−1</sup> at temperatures below 200 °C.<sup>[23,24]</sup> After an activation period (25 min), during which free surface sites for reaction are likely generated by partial ligand removal (see below), stable conversion is maintained over hours (the longest test was performed over 50 h).

[\*] B. Jürgens, Dr. H. Borchert,<sup>[†]</sup> P. Sonström, Dr. V. Zielasek, Prof. M. Bäumer  
Institute of Applied and Physical Chemistry, University Bremen  
Leobener Strasse NW2, 28359 Bremen (Germany)  
Dr. A. Pretorius, Dr. M. Schowalter, K. Gries, Prof. A. Rosenauer  
Institute of Solid State Physics, University Bremen  
Otto-Hahn-Allee, 28359 Bremen (Germany)  
Dr. K. Ahrenstorf, Prof. H. Weller  
Institute of Physical Chemistry, University Hamburg  
Grindelallee 117, 20146 Hamburg (Germany)

[†] Present Address: Department of Physics, Energy and Semiconductor Research Laboratory, University of Oldenburg  
Carl-von-Ossietzky-Strasse 9-11, 26129 Oldenburg (Germany)

[\*\*] We are grateful to the Fonds der Chemischen Industrie for financial support. We thank Prof. K. Al-Shamery (University Oldenburg) for valuable discussions, Dr. G. Nyce (Lawrence Livermore National Lab (USA)) for critical reading of the manuscript, and Dr. X. Wang for the preparation of the Pt nanoparticles.

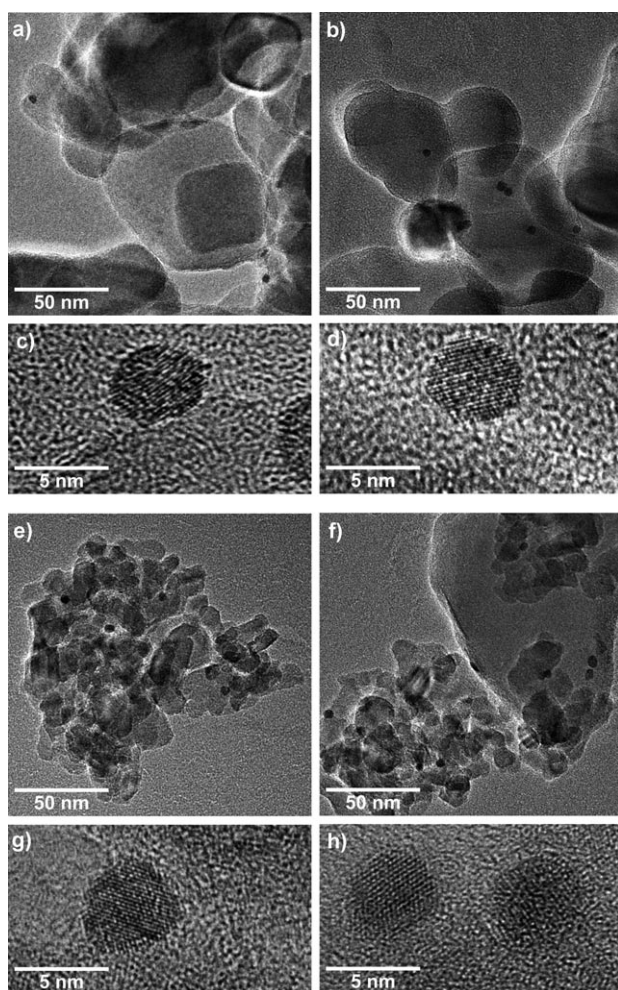


**Figure 1.** Overview (a,b,e,f) and high-resolution (c,d,g,h) TEM (HRTEM) images of NiPt nanoparticles on MgO (a–d) and Al<sub>2</sub>O<sub>3</sub> (e–h). The nanoparticles are crystalline before (left column) and after (right column) catalysis. No structural differences are discernible.

IR spectra of the catalysts were recorded under reaction conditions at 170 °C to study the differences between the two catalysts in more detail (Figure 3). Starting with the magnesia-supported particles (Figure 3a), a band appears at around 2040 cm<sup>−1</sup> shortly after the start of the reaction. As a band at the same wavenumber was detected in a previous study on colloidal Pt nanoparticles, it is tempting to assign absorption to CO linearly bonded to metallic Pt.<sup>[14]</sup> However, terminally adsorbed CO on Ni should give bands in a similar spectral region,<sup>[25]</sup> so that a corresponding contribution cannot be excluded. The increase over time of the CO<sub>2</sub> gas-phase absorption bands (2290–2390 cm<sup>−1</sup>) confirms the catalytic activity of the particles. The concomitant decrease of the signal at 2040 cm<sup>−1</sup> indicates the effective removal of adsorbed CO by the reaction.

Two other features in the spectrum are conspicuous. In the C–H stretching region (2850–3000 cm<sup>−1</sup>), strong negative bands occur, which point to a loss of ligands. However, as in a previous study on pure Pt nanoparticles,<sup>[14]</sup> the intensity of the IR bands in spectra not referenced to the background

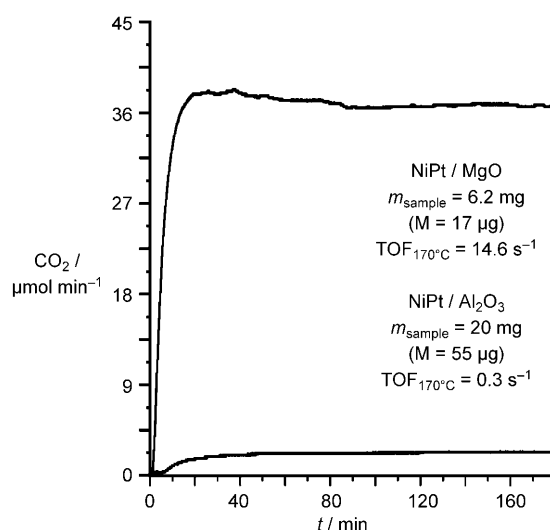


**Figure 2.** Development of the catalytic activity for CO oxidation of magnesia- and alumina-supported colloidal NiPt particles (gas feed: 0.017 mL s<sup>−1</sup> CO + 0.16 mL s<sup>−1</sup> O<sub>2</sub> + 0.65 mL s<sup>−1</sup> N<sub>2</sub>) as well as turnover frequencies (TOF; i.e., number of CO<sub>2</sub> molecules obtained per surface site and second) at 170 °C. M: metal content.

spectrum did not completely vanish, meaning that only a fraction of the ligands is removed under the reaction conditions. Furthermore, a strong signal develops at 2190 cm<sup>−1</sup>, which at first sight seems to point to CO adsorption on oxidized Ni sites.<sup>[26]</sup> However, experiments with the pure ligands deposited on the same support clearly revealed that the signal must originate from a reaction of the ligand oleylamine with the magnesia support (see Figure 3e). Although the mechanism of the interaction is unclear, the position of the band would be consistent with nitrile formation. This unexpected finding also implies that at least a partial spillover of the ligands from the particles to the support takes place. To check this hypothesis, we recorded a second series of IR spectra for the particles at the same temperature and CO partial pressure but without oxygen in the gas feed (Figure 3c). The data show that the spillover process is thermally activated, since a similar increase of the band at 2190 cm<sup>−1</sup> is detected as under reaction conditions. Concomitantly, the amount of CO adsorbed on the particles increases, as inferred from the corresponding absorption band. It is interesting that weaker negative signals develop in the region of the C–H stretching frequencies without oxygen than with oxygen at 170 °C. Evidently, the loss of ligands in a CO/O<sub>2</sub> atmosphere is largely due to oxidative decomposition rather than thermal desorption.

The alumina-supported particles show several important differences relative to the magnesia-supported particles. First, the signal at 2050 cm<sup>−1</sup> for CO adsorbed on the particles is rapidly and strongly blue-shifted under reaction conditions, resulting in a double feature at 2080/2110 cm<sup>−1</sup> (Figure 3b).<sup>[27]</sup> Such changes are not observed without oxygen (see Figure 3d), so partial surface oxidation of the particles is a plausible explanation for the drastic shift.<sup>[28]</sup> This process is accompanied by an increase in the absorption band rather than a decrease as detected for the magnesia-supported

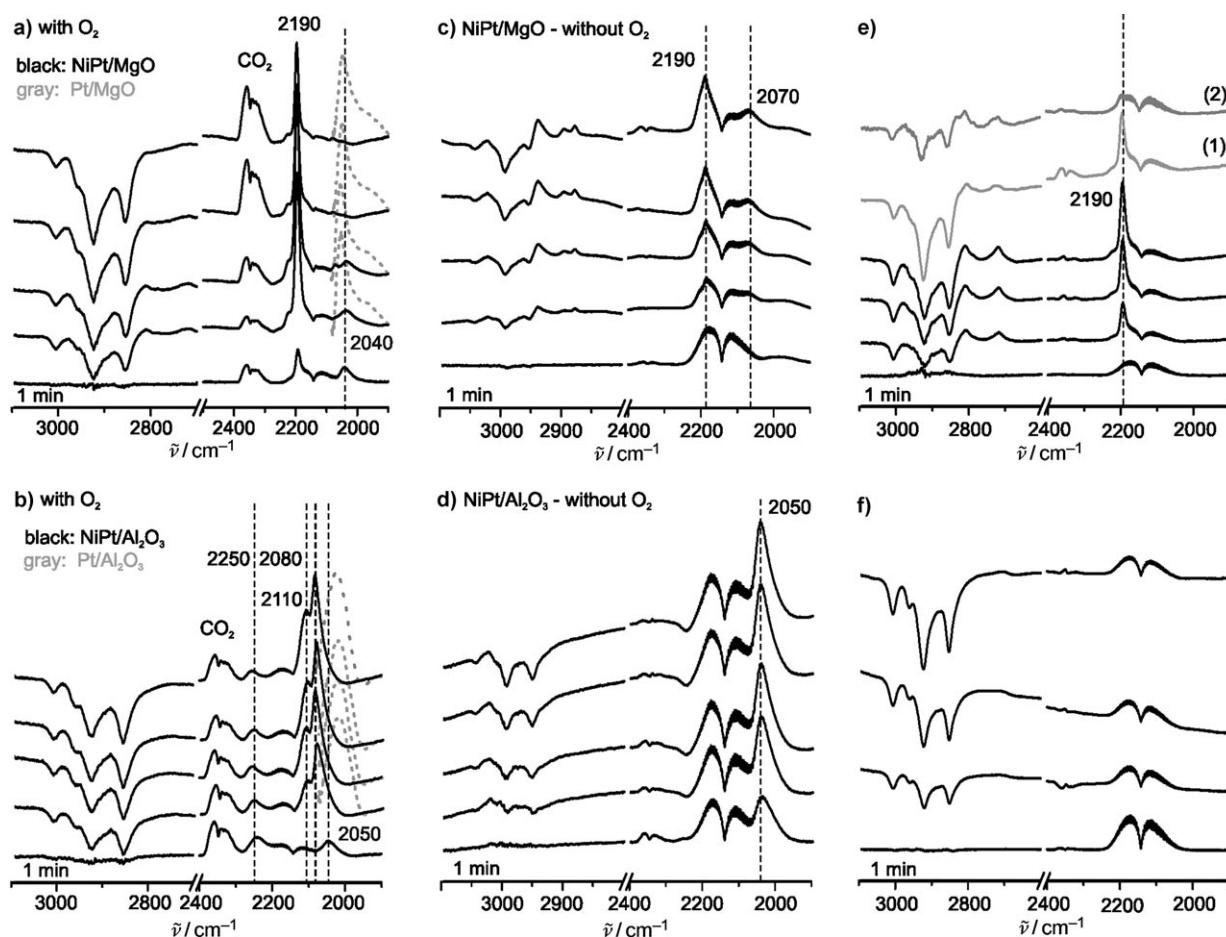


**Figure 3.** In situ IR spectra recorded at 170 °C as a function of time for NiPt colloidal particles deposited on magnesia and alumina under reaction conditions of CO oxidation. The first spectra in all series were taken after 1 min, all subsequent spectra after 60 min each. After 4 h the spectra show only marginal changes. a,b) 0.017 mL s<sup>-1</sup> CO + 0.16 mL s<sup>-1</sup> O<sub>2</sub> + 0.65 mL s<sup>-1</sup> N<sub>2</sub>; the gray dotted spectra were obtained for oleylamine-stabilized Pt particles deposited on the same supports and investigated under the same conditions. c,d) Spectra collected without O<sub>2</sub> (0.017 mL s<sup>-1</sup> CO + 0.82 mL s<sup>-1</sup> N<sub>2</sub>). e,f) Spectra of the pure ligands (mixtures of oleylamine and oleic acid) on the same supports shown for comparison. The gray spectra in (e) were recorded for pure oleylamine (1) and pure oleic acid (2) after 1 h under reaction conditions.

particles. This result is consistent with the low catalytic activity of the system, which leads to a higher CO coverage on the particle surface.

Second, the signal at 2190 cm<sup>-1</sup> is absent, and another signal is present in the spectra at 2250 cm<sup>-1</sup>. Neither of the two bands is observed when pure ligands are deposited on alumina (Figure 3 f). Notwithstanding the possibility of a spillover process taking place on alumina as well (see below), no specific reaction between support and ligands occurs in this case, and the absorption at 2250 cm<sup>-1</sup> must be related to CO adsorption on the particles. The existence of such a blue-shifted signal provides further evidence for surface oxidation of the particles. (Bands in the region of 2250 cm<sup>-1</sup> have been assigned to Pt<sup>2+</sup> carbonyl species.)<sup>[26]</sup>

Comparison of the TEM images of the two systems before and after catalysis (Figure 1) reveals no structural changes. Therefore, sintering and specific (chemical) interactions with one of the supports, which should result in changes of the particle shape, can be excluded as explanations for the large differences in activities of the magnesia- and alumina-supported particles. The particles are still crystalline and

EDX analysis provided no evidence for a change in composition. The latter observation rules out diffusion of Ni into the support and spinel formation, which was reported as a possible cause for deactivation for another bimetallic system.<sup>[18]</sup> Thus, the inferior catalytic activity of the alumina-supported nanoparticles must result from the modified surface chemistry detected by IR spectroscopy. In particular, the oxidation of Ni—although not directly detectable in the IR spectra—may result in the loss of the bimetallic surface composition, along with its superior catalytic activity.

To test this hypothesis, control experiments were carried out with pure Pt nanoparticles capped with oleylamine ligands. In this case, very low conversion rates at 170 °C were obtained on both supports (TOF = 0.1 s<sup>-1</sup> (on Al<sub>2</sub>O<sub>3</sub>); 0.2 s<sup>-1</sup> (on MgO)), although no indication of changes in the surface chemistry were detected by IR spectroscopy with our reaction conditions (see gray dotted signals in Figure 3 a,b). This result proves the beneficial effect of Ni for the low-temperature activity, which is apparently lost for the alumina-supported system. A possible explanation for why Ni is not oxidized in the case of magnesia-supported NiPt is the partial



protection by residual ligands on this support. As alumina is more acidic than magnesia, a higher degree of spillover of the Lewis-basic ligands on alumina is likely (although in this case a chemical reaction between ligands and support is not involved). This spillover would lead to less-protected particles, which are more easily affected by the oxidative reaction conditions.

In summary, we have shown that highly active and structurally well-defined catalysts can be prepared by depositing colloidal nanoparticles on suitable supports. No prior thermal or oxidative treatment (calcination) is needed to obtain immediate activity. Nevertheless, the support can play a decisive role. Our results suggest that residual ligands may have a protecting effect and that the ligands may be removed from the surface of the particles onto the support by spillover processes to a different degree.

### Experimental Section

The colloidal synthesis of the NiPt nanocrystals stabilized with oleic acid and oleylamine ligands is described in detail elsewhere.<sup>[16]</sup> To prepare oxide-supported powder catalysts, colloidal solution was dropped onto  $\gamma$ -Al<sub>2</sub>O<sub>3</sub> (Alfa Aesar, 255 m<sup>2</sup> g<sup>-1</sup>) or MgO (23.5 m<sup>2</sup> g<sup>-1</sup>), and the suspension was subsequently dried. For comparison, pure Pt particles, prepared according to reference [17] and subsequently capped by oleylamine, were deposited onto the same supports. IR spectroscopy was performed in diffuse reflection geometry (DRIFTS) with a Biorad FTIR spectrometer. Samples were pressed into pellets and investigated in a heatable reaction cell equipped with a controlled gas supply system for in situ studies. All spectra were recorded with a resolution of 2 cm<sup>-1</sup> under continuous gas flow with Ar as carrier gas. The catalytic performance of the different catalysts was examined in laboratory reactors connected to a controlled gas supply system and photometric detectors (Hartmann & Braun URAS 10E and URAS 3G) for CO/CO<sub>2</sub> analysis of the exhaust gas. Precautions were taken to avoid mass-transport limitations: the powder catalysts were pressed and sieved into 0.45–0.71 mm grains. The NiPt/MgO sample (6.2 mg; 17  $\mu$ g total metal content) or the NiPt/Al<sub>2</sub>O<sub>3</sub> sample (20 mg; 55  $\mu$ g metal content) were then mixed with quartz (150 mg; 0.4–0.8 mm). The mixture was then placed between quartz wool into the reactor. Transmission electron microscopy (TEM) was performed on a TITAN 80/300 (FEI) instrument equipped with a field emission gun (FEG), a C<sub>s</sub>-image corrector, and operated at 300 kV. The number of surface metal atoms, which was required to calculate the turnover frequencies, was estimated from the particle size and lattice parameter by assuming a spherical model.

Received: May 9, 2008

Published online: October 16, 2008

**Keywords:** colloids · heterogeneous catalysis · nanoparticles · oxidation · supported catalysts

- [1] T. Hyeon, *Chem. Commun.* **2003**, 927.
- [2] E. V. Shevchenko, D. V. Talapin, N. A. Kotov, S. O'Brien, C. B. Murray, *Nature* **2006**, 439, 55.
- [3] S. H. Joo, S. J. Choi, I. Oh, J. Kwak, Z. Liu, O. Terasaki, R. Ryoo, *Nature* **2001**, 412, 169.
- [4] A. Taguchi, F. Schüth, *Microporous Mesoporous Mater.* **2005**, 77, 1.
- [5] J. Cao, C. Du, S. C. Wang, P. Mercier, X. Zhang, H. Yang, D. L. Akins, *Electrochem. Commun.* **2007**, 9, 735.
- [6] D. Astruc, F. Lu, J. R. Aranzas, *Angew. Chem.* **2005**, 117, 8062; *Angew. Chem. Int. Ed.* **2005**, 44, 7852.
- [7] R. Narayanan, M. A. El-Sayed, *J. Phys. Chem. B* **2005**, 109, 12663.
- [8] C. A. Stowell, B. A. Korgel, *Nano Lett.* **2005**, 5, 1203.
- [9] J. W. Yoo, D. Hathcock, M. A. El-Sayed, *J. Phys. Chem. A* **2002**, 106, 2049.
- [10] M. Comotti, W.-C. Li, B. Splithoff, F. Schüth, *J. Am. Chem. Soc.* **2006**, 128, 917.
- [11] A. Singh, B. D. Chandler, *Langmuir* **2005**, 21, 10776.
- [12] V. Pérez-Dieste, O. M. Castellini, J. N. Crain, M. A. Eriksson, A. Kirakosian, J.-L. Lin, J. L. McChesney, C. T. Black, C. B. Murray, F. J. Himpsel, *Appl. Phys. Lett.* **2003**, 83, 5053–5055.
- [13] B. Gehl, A. Frömsdorf, V. Aleksandrovic, T. Schmidt, A. Pretorius, J. I. Flege, S. Bernstorff, A. Rosenauer, J. Falta, H. Weller, M. Bäumer, *Adv. Funct. Mater.* **2008**, 18, 2398–2410.
- [14] H. Borchert, D. Fenske, J. Kolny-Olesiak, J. Parisi, K. Al-Shamery, M. Bäumer, *Angew. Chem.* **2007**, 119, 2981; *Angew. Chem. Int. Ed.* **2007**, 46, 2923.
- [15] K. M. Bratlie, H. Lee, K. Komvopoulos, P. Yang, G. A. Somorjai, *Nano Lett.* **2007**, 7, 3097.
- [16] K. Ahrenstorf, O. Albrecht, H. Heller, A. Kornowski, D. Görlitz, H. Weller, *Small* **2007**, 3, 271.
- [17] Y. Wang, J. Ren, K. Deng, L. Gui, Y. Tang, *Chem. Mater.* **2000**, 12, 1622.
- [18] C. Kwak, T.-J. Park, D. J. Suh, *Appl. Catal. A* **2005**, 278, 181.
- [19] M. Alnot, A. Cassuto, R. Ducros, J. J. Ehrhardt, B. Weber, *Surf. Sci.* **1982**, 114, L48.
- [20] K. Teruuchi, H. Habazaki, A. Kawashima, K. Asami, K. Hashimoto, *Appl. Catal.* **1991**, 76, 79.
- [21] A. Siani, O. S. Alexeev, B. Captain, G. Lafaye, P. Marécot, R. D. Adams, M. D. Amiridis, *J. Catal.* **2008**, 255, 162.
- [22] J. Greeley, J. K. Nørskov, *Surf. Sci.* **2005**, 592, 104.
- [23] A. K. Santra, D. W. Goodman, *Electrochim. Acta* **2002**, 47, 3595.
- [24] A. Bourane, D. Bianchi, *J. Catal.* **2004**, 222, 499.
- [25] U. Heiz, *Appl. Phys. A* **1998**, 67, 621.
- [26] K. I. Hadjiivanov, G. N. Vayssilov, *Adv. Catal.* **2002**, 47, 307.
- [27] A major peak with a shoulder at higher wavenumber was also observed by Bourane and Bianchi for CO adsorption on conventional alumina-supported Pt particles (A. Bourane, D. Bianchi, *J. Catal.* **2003**, 218, 447). The reported wavenumbers, however, were somewhat lower (main peak at 2070 cm<sup>-1</sup>, shoulder at 2085 cm<sup>-1</sup> for particles of similar size) than in our study. In fact, the shoulder at 2110 cm<sup>-1</sup> in Figure 3 is close to the frequencies reported for CO adsorption on Pt<sup>+</sup> or Pt<sup>2+</sup>.<sup>[26]</sup>
- [28] P. J. Lévy, V. Pitchon, V. Perrichon, M. Primet, M. Chevrier, C. Gauthier, *J. Catal.* **1998**, 178, 363.